Dynamic compaction of powders by an oblique detonation wave in the cylindrical configuration

E. P. Carton
TNO-Prins Maurits Laboratory, Post Office Box 45, 2280 AA, Rijswijk, The Netherlands and Laboratory for Applied Inorganic Chemistry, Delft University of Technology, Post Office Box 5045, 2600 GA, Delft, The Netherlands

H. J. Verbeek and M. Stuivinga
TNO-Prins Maurits Laboratory, Post Office Box 45, 2280 AA, Rijswijk, The Netherlands

J. Schoonman
Laboratory for Applied Inorganic Chemistry, Delft University of Technology, Post Office Box 5045, 2600 GA, Delft, The Netherlands

(Received 20 September 1996; accepted for publication 31 December 1996)

A new method has been applied to dynamically compact ceramic powders in the cylindrical configuration. In this method, a converging oblique detonation is used instead of the sliding detonation used in the standard method. The oblique detonation is generated by a configuration using two explosive layers. X-ray flash photographs have been made that show the detonation and shock fronts in both the standard and new configuration. In the present article, the shock wave and particle velocities in the B_4C powder have been calculated using the shock and detonation angles obtained from the photographs in combination with the measured detonation velocity. In the two-layer configuration, the pressure applied to the powder was increased by a factor of 3.5 compared to the one-layer configuration, in agreement with calculations. The working principle of the two-layer configuration is discussed and compared with a computer simulation of the process.
 [S0021-8979(97)04407-1]

I. INTRODUCTION

A. Dynamic compaction of powders

Dynamic compaction, i.e., compaction by a shock wave,[1] is an alternative way to consolidate plastic, ceramic, and metallic powders and combinations thereof. For some materials, it is the only way to obtain products without deterioration of the special properties of the starting materials. For example, products of rapidly solidified powders (RSP)[2] can be formed with this technique since cooling rates that occur in dynamic compaction are at least as high as they were during their production process. Since no sintering aids are needed, the process is also interesting for the compaction of strongly covalent bonded ceramics,[3,4] because their intrinsic high temperature strength remains unaffected.

Also powders have been modified by shock wave propagation in order to increase their reactivity (catalysts[5]) or sinterability.[6] The principle behind the shock modification of powders is the generation of a high concentration of defects in the lattice (especially vacancies and dislocations), by the propagating shock wave. The high pressures and strain rates that occur in dynamic compaction of powders can result in phase transformation of the material. This phenomenon is used in the synthesis of nonequilibrium phases as w-BN[7] and diamond[8] (the latter even on a commercial basis).

Research activities in the dynamic compaction of powders started in the 1940s.[9] To avoid the complexity of multiaxial stress and mass flows in shock waves, scientists have made use of special devices to generate plane shock waves in the material to be investigated.[10] A plane shock wave can be generated by a plane-wave lens initiating a plane detonation wave in an explosive or by the perpendicular impact of a flat projectile accelerated by a gas gun.[11] Especially with a gas gun, a great variety of shock pulses can be introduced in the target with high accuracy due to the high accuracy with which the velocity of the projectile can be measured. For large surfaces, a mouse-trap configuration is an economical alternative method.[10] Drawbacks of using plane wave techniques are the high cost of the equipment and the lack of possibilities to scale up the process. This is because in a plane shock wave there is no possibility to compensate for the energy dissipation which occurs in any shock wave. Especially in powders, shock wave propagation is accompanied by a large dissipation of energy due to the large irreversible change in specific volume occurring in the dynamic compaction process. For bulk fabrication of compacted materials, the cylindrical configuration is more convenient. In this configuration, the energy absorption is compensated by the geometrical effect of convergence of the shock wave. Prümmer has pioneered this method in the seventies.[12] This configuration can be scaled up by changing the length of the container and, although this is less straightforward, by changing its diameter.

B. Standard cylindrical configuration

In the standard cylindrical configuration, powders are compacted by an axisymmetrical shock wave initiated by the axially moving (sliding) detonation front in the surrounding explosive. The angle between the shock front in the powder and the cylinder axis is a function of the ratio between the shock wave velocity, U_s, and the detonation velocity of the explosive, D, as shown in Fig. 1:

$$\sin \alpha = U_s / D. \tag{1}$$

 0021-8979/97/81(7)/3038/8/$10.00

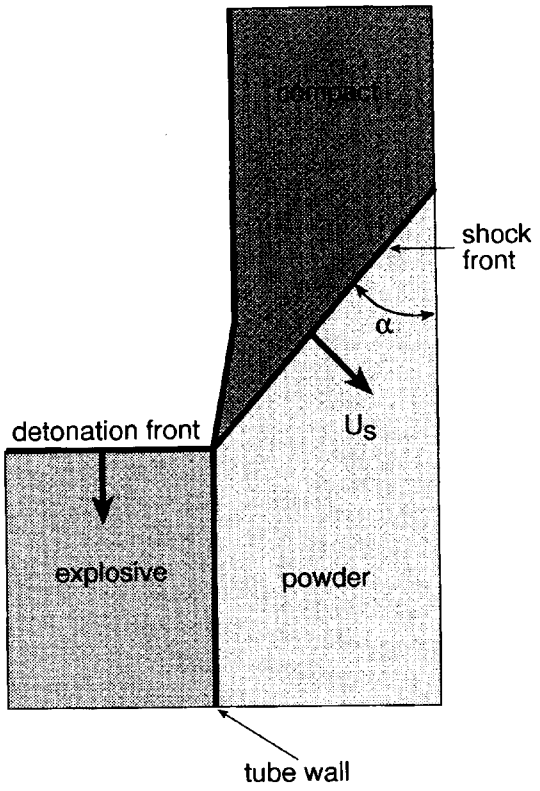

FIG. 1. Detonation front and shock front during compaction.

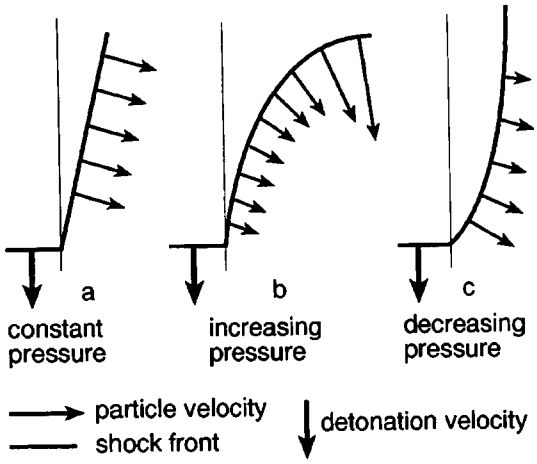

FIG. 2. Shock wave front forms in the cylindrical configuration.

Due to its radial component and to the cylindrical geometry, the shock wave converges as it propagates through the powder. The area on which the shock wave energy is acting decreases and hence the energy density increases. As a consequence, the pressure, P, and shock wave velocity, U_s, also increase. On the other hand, energy is dissipated during compaction by processes taking place in the shock front such as particle rearrangement, cracking, plastic deformation, friction, and melting. This energy dissipation results in a decreasing pressure and shock wave velocity. Whether the pressure and shock wave velocity in the powder increase or decrease depends on the relative strength of the convergence and absorption processes. If both processes just balance, the pressure and shock wave velocity are constant. From Eq. (1), it follows that, for a constant detonation velocity D, this leads to a conical shock front with an angle α, equal to arc sin (U_s/D). If one of the processes predominates the other, P and U_s will be a function of the radial position in the powder and the form of the shock wave will change (see Fig. 2).

Dynamic compaction of powders with this method is a rather inefficient process. The energy generated by the explosive is sliding by rather than directly acting upon the container (see Fig. 1). This reduces the pressure acting on the container with approximately a factor of two compared to the pressure generated with the same explosive when the detonation front strikes perpendicularly. In general, nonideal explosives with low detonation velocities (2–4 km/s) are used to avoid cracks in the compact due to rarefaction waves. The rarefaction waves originate from reflections of the shock wave at the free surface of the container. The longer pulse length of the nonideal explosive reduces the intensity of these waves.

Since the detonation pressure is quadratically proportional to the detonation velocity, pressures, obtained with low detonation velocity explosives, are limited. In order to increase the pressure acting on the container, indirect methods such as flyer tubes can be used.[13] In this case, shock waves are generated in the powder by the impact of an explosively accelerated flyer tube. During impact, higher pressures can be generated compared to the case where the detonation is acting directly on the container.

A higher pressure and a better energy efficiency can also be obtained by directing the detonation wave towards the container by using two explosive layers, as will be explained below.

C. Refraction of shock waves

Since shock waves and detonations are wave phenomena, they can be compared to other wave-phenomena like sound, light, and surface waves. All these wave phenomena have to obey the general laws of wave physics like Huygens principle and Snell's law.[14,15] We can direct a shock wave in the same way we can focus light using refraction and reflection. The direction in which a detonation is propagating through an explosive will change according to Snell's law when it passes the interface with an explosive having another detonation velocity, just like light changes its direction when traveling from one medium to another. In Ref. 15, Weinheimer gives examples in which the principles of shock wave mechanics can be derived from the science of geometrical optics. For example, Eq. (1) can be obtained directly from Snell's law (with $\theta_i=90°$):

$$\sin \theta_i/\sin \theta_r = c_i/c_r \tag{2}$$

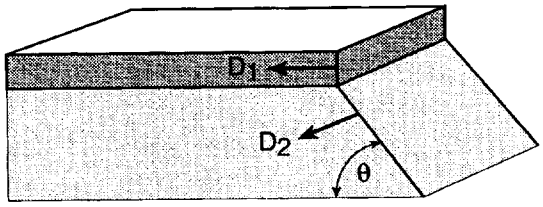

FIG. 3. Oblique detonation wave (D_2) in a plane explosive layer initiated by a faster detonation wave (D_1).

in which subscripts i and r represent the incident and refracted wave, respectively, and c is the velocity of propagation of the wave phenomenon through the medium.

If an explosive with a detonation velocity (D_1) is initiated by a faster detonating explosive (D_2), an oblique detonation front will form in the latter (see Fig. 3). The angle θ between the oblique detonation front and the interface between the two explosives is given by Eq. (1) after substitution of D_1 for U_s and D_2 for D:

$$\sin \theta = D_1/D_2. \tag{3}$$

This planar arrangement is used to investigate regular and irregular reflections of detonation and shock waves on flat surfaces.[16]

D. Two-layer configuration

Also in the cylindrical configuration an oblique detonation with angle θ will form when a layer of a fast detonating explosive (D_2) is surrounding an inner layer of explosive with a lower detonation velocity (D_1) [see Fig. 4(b)]. The detonation in the second, slower, explosive has a radial component and is converging while propagating towards the axis. This arrangement increases the efficiency of the dynamic compaction process since both the convergence of the detonation wave and the angle θ at which it strikes the container lead to an increased pressure in the powder. The pulse length of the detonation in the two-layer configuration is longer than in the case that an ideal explosive in the one-layer configuration is used, not only because a nonideal explosive with a long pulse length is used as the inner explosive but also because the detonation products of the inner explosive layer are confined by the expanding detonation products of the outer explosive layer. This is important in order to avoid (the interaction of) strong rarefaction waves that generally lead to cracking of the compact.

In this article, experiments are described during which x-ray photographs were taken that show the differences that occur using the two-layer configuration compared with the standard one-layer configuration. The organization of this article is as follows. The experimental arrangement is explained in Sec. II. Then, in Sec. III, the results of the experiments are presented. In Sec. IV, the pressures and shock wave velocities are calculated from the x-ray photographs. Computer simulations of both configurations are presented in Sec. V, followed by a discussion of the results in Sec. VI.

II. THE EXPERIMENTAL ARRANGEMENT

Experiments were performed in order to compare the standard (one layer) arrangement with the new (two layer) arrangement [see Figs. 4(a) and 4(b)]. During the experiments, x-ray photographs were taken using x-ray flashers with a flash time of 20 ns. From the photographs, both the detonation waves and the shock waves could be observed and their angles with respect to the tube axis were measured.

From experiments in which two photographs with a known time difference were taken, the detonation velocity could be determined. Triamite, a mining explosive manufactured by PRB, Belgium, was used in both the standard and the new arrangement. Its detonation velocity is measured to be 4.3 km/s. Demex 200, a sheet explosive manufactured by Royal Ordnance Inc., UK, was used in the new arrangement because of its high detonation velocity of 7.8 km/s. In both experiments, the explosives were placed in a 220-mm-long PVC cylinder with an inner diameter of 68 mm. A detonator was placed on top of the explosives at the cylinder axis. In the new arrangement, the upper part of the Demex sheet explosive was folded towards the detonator to ensure that initiation took place in the Demex sheet first. In Table I, the experimental details are given.

The powder to be compacted was boroncarbide (B_4C), a hard to sinter, strongly covalent bonded ceramic with a theoretical maximum density (TMD) of 2.52 mg/mm^3 (manufactured by ESK, Germany). In order to avoid spiral cracks, a trimodal powder mixture with a high starting density (ρ_0) was used. Three particle sizes (~4, 16–49, and 100–150 μm) with a mass ratio of 10:28:62 were mixed in a turbulator for 20 min. A 120-mm-long aluminum cylinder (outer diameter 34.8 mm and wall thickness 2.3 mm) was filled with the powder mixture by mechanical tapping and uniaxial pressing at 20 MPa. In this way, a starting density of 65.5% (TMD) was obtained.

After the experiments, the aluminum cylinder was cut perpendicularly to the tube axis in order that the compacted powder could be analyzed microscopically.

III. EXPERIMENTAL RESULTS

A. Measured angles

In Fig. 5, an x-ray photograph of the experiment with the standard arrangement is given. The grazing detonation front (θ=90°) in Triamite is clearly visible and also the (conical) shock front in the powder can be seen.

Figure 6 shows the new arrangement during the explosive compaction process. The sheet detonation initiates the detonation in Triamite and an oblique detonation front is formed in the latter. The detonation angle θ is 34±2 deg as could be expected from the ratio of the detonation velocities (see Table I). Due to the nonideal initiation of the bent Demex, its detonation front is not at the same axial position left and right from the aluminum cylinder. Also the shock wave front in the powder is visible in Fig. 6.

The experiments were performed to show the working principle of the configurations and are not intended to be a measuring technique. Nevertheless, using the angles (α,β,θ) and the jump relations for shock waves (conservation of

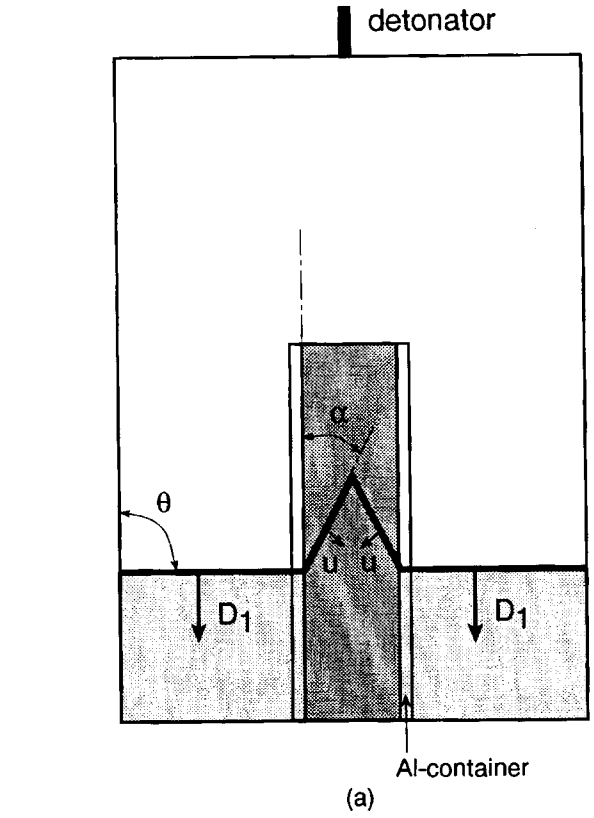

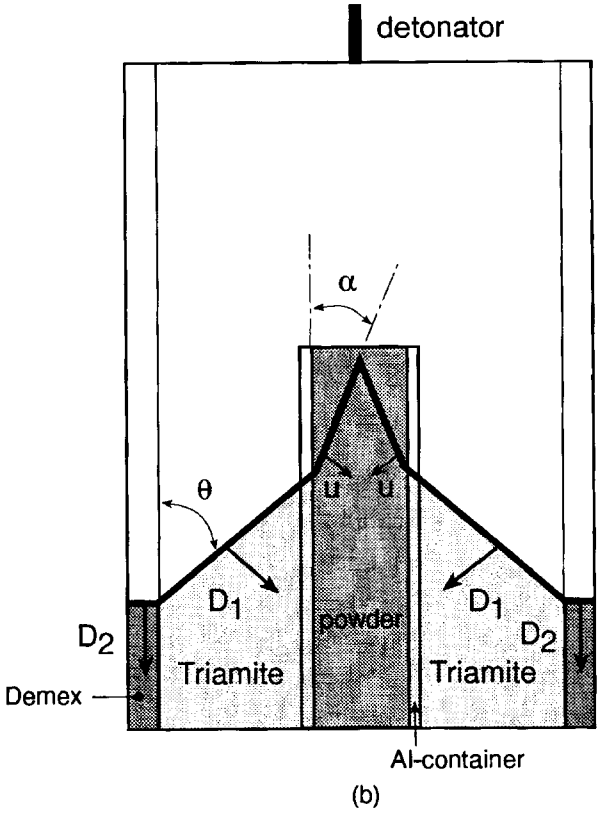

FIG. 4. (a) Shock fronts in standard one-layer configuration. (b) Shock fronts in new two-layer configuration.

TABLE I. Experimental details.

Arrangement	One layer	Two layer	
Explosive	Triamite	Triamite	Demex
Layer thickness (mm)	16.6	13.6	3.0
D (km/s)	4.3±0.1	4.3±0.2	7.8±0.2
θ	90°±1°	33.5°±1° [a]	···
ρ_0 (% TMD of B_4C)	65.5	65.5	···

[a]Calculated using Eq. (3).

mass, momentum and energy), it is possible to calculate the shock wave and particle velocity of the initial shock wave. Using these, the pressure and density of the powder can be calculated. For higher accuracies, measurements using specific sensors should be used. In Table II, the measured angles (α,β,θ) are given for both arrangements [see Figs. 5(b) and 6(b)].

B. B_4C compacts

In Figs. 7(a) and 7(b), the cross sections of the cylinders after dynamic compaction are shown. The boroncarbide

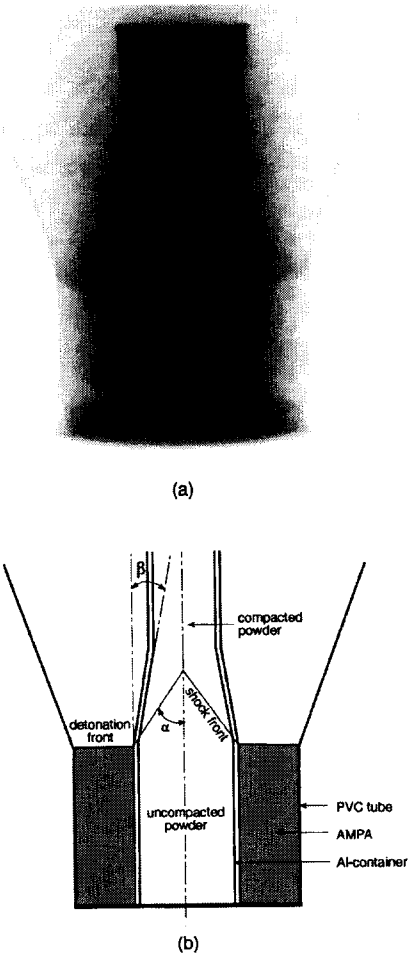

FIG. 5. (a) Flash x-ray photograph of powder compaction in standard configuration. (b) Schematic picture of angles visible in x-ray photograph.

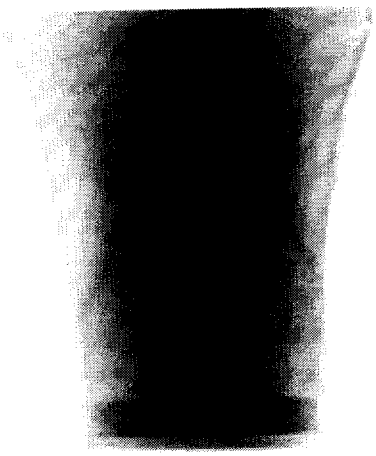

(a)

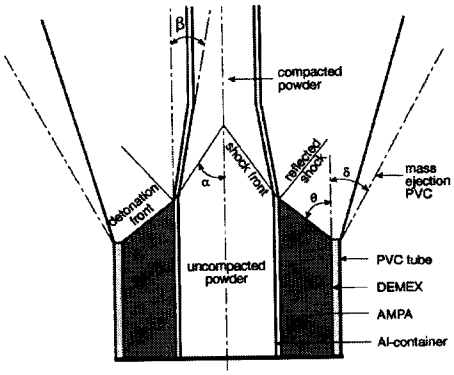

(b)

FIG. 6. (a) Flash x-ray photograph of powder compaction in two-layer configuration. (b) Schematic picture of angles visible in x-ray photograph.

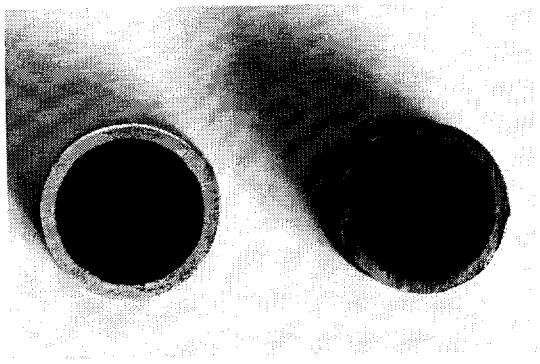

(a) (b)

FIG. 7. (a) Cross section of B_4C compact obtained with one-layer configuration. (b) Cross section of B_4C compact obtained with two-layer configuration.

powder, compacted with the standard arrangement [Fig. 7(a)] shows a homogeneous material. Apparently the pressure and shock wave velocity were approximately constant over the radius, like in Fig. 2(a). The compaction process has not been able to densify the powder to full density. The density of the material, calculated from the reduction in diameter of the cylinder, is 86% TMD and no bonding, apart from mechanical interlocking, has occurred. The material compacted in the two-layer arrangement is inhomogeneous [Fig. 7(b)]. In the center, an area with a diameter of 6 mm shows bonding and has a high density. The cracks shown in Fig. 7(b) are probably the result of differences in expansion of the material in the center and the periphery during pressure release.

IV. CALCULATIONS

A. Calculations from the experimental results

In the standard configuration, the shock wave velocity in the powder can be calculated from the angle α using Eq. (1) (see Table II).

In the two-layer configuration, the shock wave velocity in the powder can be found from the combination of Eqs. (1) and (3), resulting in:

$$U_s = D_2 \sin \alpha \tag{4}$$

in which D_2 is the measured detonation velocity of the Demex sheet explosive. The particle velocity (u_p) can be obtained from the angles α and β, where β is the angle between the cylinder axis and the interface between the powder and the container wall (see Figs. 5 and 6). For a stationary condition, in which the form of the shock front (see Fig. 2) moves down with the axial velocity D, the powder/container interface moves with velocity u_i:

$$u_i = D \sin \beta. \tag{5}$$

The direction of the particle velocity of the powder is parallel to the direction of the shock wave velocity (U_s). This means that we have to take into account the difference in direction of propagation between the interface and the particle velocity of the powder (u_p). The difference in direction of propagation between the two is ($\alpha-\beta$), and the particle velocity of the powder is:

$$u_p = u_i/\cos(\alpha-\beta) = D \sin \beta/\cos(\alpha-\beta). \tag{6}$$

From the jump relations (conservation of mass, energy, and momentum), we can derive an equation relating the pres-

TABLE II. Experimental results.

	α (°)	β (°)	θ (°)	U_s (km/s)	u_p (km/s)	P (GPa)
One layer	36±1	7±2	90±1	2.5±0.1	0.6±0.1	2.5±0.6
Two layer	42±4	6±2	34±2	5.2±0.5	1.0±0.2	9±2

sure in the shock wave to the shock wave velocity (U_s), particle velocity, and the starting density (ρ_0):

$$P=\rho_0 U_s u_p. \tag{7}$$

The calculated shock wave pressures for both arrangements are shown in Table II. The pressure in the two-layer arrangement appears to have increased with a factor of approximately 3.5 with respect to the one-layer arrangement.

B. Calculations from theory

The increase in shock wave pressure obtained with the two-layer configuration compared to the standard one-layer configuration can be explained by both the obliqueness and the convergence of the detonation wave.

The oblique detonation wave is partly directed towards the cylinder, in contrast to the grazing detonation in the case of the one-layer configuration. The pressures, resulting from the impact of an oblique shock wave on the interface between two materials, can be calculated in the same way as for the perpendicular impact of a shock wave by using the perpendicular component of the particle velocities. The resulting pressure P_2 in the impacted material is then given by the relation:

$$P_2=P_{CJ}(1+\cos\theta)I_2/(I_1\cos\alpha+I_2), \tag{8}$$

where P_{CJ} is the Chapman–Jouguet pressure of the impacting detonation wave, θ is the angle between the impacting shock front, and the interface and α is the angle of the shock front in the impacted material. I_1 and I_2 are the shock impedances of the two materials ($\rho_0 U_s$), which are assumed to be independent of pressure here.

When we apply Eq. (8) to the cases of an oblique detonation wave and a grazing detonation wave, it follows that the pressures are 1.30 and 0.52 P_{CJ}, respectively. The pressure in the two-layer configuration is increased with a factor of 2.50 by this mechanism.

When a shock wave propagates in a cylindrical geometry at an oblique angle to the axis, its energy density will increase when it approaches the axis due to the decreasing surface area. An estimate of the size of this effect has been given by Boogerd.[17] In his calculations, it is assumed that the pulse length is a constant and the energy density change is given by:

$$dE/dr=-E/S.dS/dr, \tag{9}$$

where E is the energy of the shock wave per unit mass, S is the surface of the shock wave, and r is the average distance to the cylinder axis. Using $S=2\pi rh$, where h is an infinitesimal height of the shock front, it follows that $E\sim 1/r$. From the jump relations, we find

$$E\sim P(V_0-V)\sim 1/r, \tag{10}$$

where P is the pressure of the shock wave and V_0 and V are the specific volumes, respectively, before and behind the front of the shock wave.

In order to be able to apply this equation to a converging detonation in Triamite, we need a relation for the Hugoniot of the explosive. Such an expression has been estimated with use of the computer code Tiger,[18] yielding the result:

$$P\approx 15.91-24.68\ 1/V+11.82\ 1/V^2. \tag{11}$$

From Eqs. (9) and (10), using the assumption that the pressure at the interface with the sheet explosive is equal to the Chapman–Jouguet (CJ) pressure of Triamite (5.14 GPa as obtained from Tiger), we can now calculate the pressure at the interface with the aluminum cylinder. It then follows that since the diameter of the shock front decreases from 62.0 to 34.8 mm, the pressure increases to a value of 7.14 GPa, an increase of 38% over the CJ value.

Therefore, the total increase in pressure from both mechanisms is calculated to be a factor of 3.45.

V. SIMULATIONS

Computer simulations have also been carried out for both the one- and two-layer configuration. With these calculations, it is possible to test our ideas about the propagation and reflection of the shock waves, occurring in these configurations, and to examine the resulting values of the shock wave velocity, the shock wave pressure, and the compression. The calculations have been performed with the use of the hydrocode Autodyn.[19] To describe the shock behavior of the ceramic powder, use has been made of the porous model, intrinsic to Autodyn. Unfortunately, the current porous model in Autodyn is a very simple one and is not very reliable especially for high pressures such as that which occur near the axis of the tube. Another problem with carrying out the calculations is that the material properties of porous B_4C, which are necessary as input data for the code, are not very well known. An estimate of the material properties has been made, using as a starting point the model for the Hugoniot of porous materials, developed by Boogerd *et al.*[20] and adjusted to comply with the intrinsic porous model. In this way, a material description was obtained to give a good description of the shock behavior of the material, except near the center of the tube.

As an example of the results of the simulations in Fig. 8, a pressure contour plot is shown of the compaction process, taking place in the two-layer configuration. Although the absolute values of the pressure in the figure are not very reliable, the appearance of the figure is in good agreement with the x-ray radiograph of this configuration (shown in Fig. 6) and it also shows how the pressure increases when the shock wave travels in the direction of the axis, both in the explosive and in the powder. In the center of the porous material around the axis, a region with a very high pressure develops, with a value well above the Hugoniot elastic limit for solid B_4C (19.4 GPa).[21] This high pressure region has the appearance of a Mach stem, but this is probably due to the deficiencies of the porous model at these pressures, since experimentally no evidence is seen of the occurrence of a Mach stem. The angle of the shock front in the powder agrees with the experimentally observed one within a few degrees (see Table II and III). The same applies to the simulation of the one-layer configuration (not shown here, see Table III). Although the absolute values of the pressures are not very reliable, it appears that the values, reached in the two-layer configuration, are several times as high as in the one-layer configuration, in agreement with the experimental results.

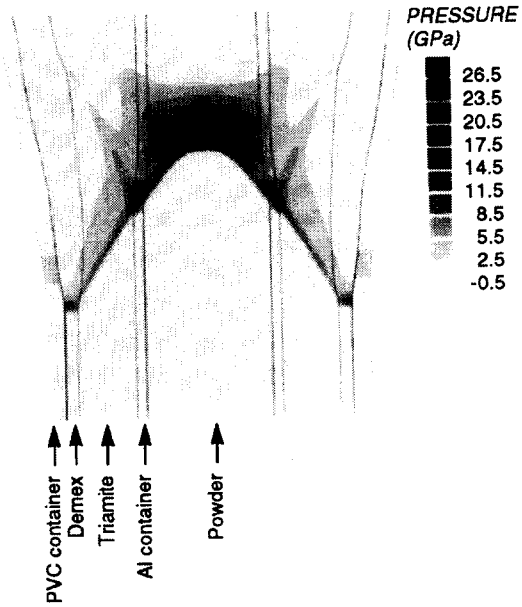

FIG. 8. Pressure contours in the two-layer configuration, obtained from the computer simulation.

VI. DISCUSSION

A. The pressure increase

From Table II, we see that the shock wave pressure in the powder using the two-layer arrangement is increased by a factor of 3.5 with respect to the pressure in the one-layer arrangement. Both the obliqueness and the convergence of the detonation wave contribute to this effect:

(i) The oblique detonation wave in the new arrangement is partly directed towards the container, in contrast to the grazing detonation in the case of the standard arrangement. Using the detonation angle (θ=34°), the pressure was calculated to increase by a factor of 2.50. Shtertser[22] calculated that it is not necessary to lower θ to 0 deg for the optimum result. Angles smaller than 30 deg give already an almost maximum increase in pressure. The detonation angle can easily be controlled by changing the ratio of detonation velocities of the two explosives.

(ii) Since the oblique detonation wave is converging towards the axis of symmetry, its energy density and hence its pressure and detonation velocity will increase as it travels through the explosive, a similar process as occurring for the shock wave in the powder. The dimensions of the configuration (the inner and outer diameter of the inner explosive layer) determine the amount of convergence of the detonation. Calculations (see Sec. IV B) showed that the convergence in the presently used two-layer arrangement has led to a pressure increase by a factor of 1.38.

The above explanations together account for a pressure increase with a factor of 3.45 which is in good agreement with the experimental results.

Another benefit of the two-layer configuration is that although high pressures are generated in the powder, the pulse length of the shock wave is longer than in the case of the one layer configuration using a high explosive. This is because in the two-layer configuration a nonideal explosive with a long pulse length is used as the inner explosive layer and furthermore the expansion of detonation products of the inner explosive is hindered by the expansion of the detonation products of the outer high explosive. The latter can be seen in Fig. 8 in which a line is drawn that separates the expanding detonation products of both explosives. The longer pulse length reduces the intensity of the rarefaction waves and therefore reduces the danger of cracking that could occur when the rarefaction waves interact.

B. Regular/irregular reflection

From Fig. 6, it is clear that the reflection of the oblique detonation wave at the container wall is a regular reflection because the shock front in the Triamite and the front of the reflected wave meet at the container wall. In the case of an irregular reflection, the intersection of both waves would occur in the explosive and at their intersection they would join a third shock wave, a so-called Mach stem.[23]

Although in the experiments, described here, a Mach stem apparently does not occur, it is quite possible that it will occur under only slightly different circumstances, e.g., when the detonation angle becomes larger than some, pressure dependent, critical angle.[23] For instance, in experiments of Adamec *et al.*[16] for aluminum and steel layers, irregular reflection was found to occur when θ became 39 (carbon steel) and 41° (Al), respectively. In our experiments, the detonation angle in the two-layer experiment was 34±2°, while θ_c will probably be larger than in the above-mentioned situations, since the large compressibility of the powder leads to an increase in θ_c.[24] Furthermore, in the case that an irregular reflection would occur, pressure would still be expected to be increased while also the benefit of the long pulse length would still be present.

C. Mass ejection

Another feature to be seen in the x-ray photograph of Fig. 6 is a straight line at the outer surface of the PVC cylinder that contained the explosives. This line is not visible in the one-layer configuration (Fig. 5). The angle γ (14°) of the line with respect to the axis of the container suggests a ve-

TABLE III. Results of computer simulation.

	α (°)	β (°)	θ (°)	ρ_{final} (% TMD)	
One layer	41±1	6±1	90±1	88.9	(86)[a]
Two layer	36±1	6.5±2	31±1	89.3	···

[a]Experimental result.

locity of 1.9 km/s. The fact that it is visible on the x-ray photograph can only be explained by a high density material escaping from the surface of the PVC container wall. This process of mass ejection from a free surface has been observed before[25–27] and occurs when a strong shock wave is reflected in vacuum or in air.

VII. CONCLUSIONS

A two-layer configuration has been applied for the dynamic compaction of powders in the cylindrical configuration. In this configuration, an oblique converging detonation front occurs the angle of which is controlled by the ratio of the detonation velocities of the two explosives used. Also the amount of convergence of the detonation wave can be controlled by the inner and outer diameter of the inner explosive. The pressures achieved with this two-layer configuration are considerably higher than those achieved with the standard one using the same explosive. The pressure increase was determined from measurements of the shock and detonation angles which were visualized by flash x-ray photography.

Both the obliqueness and the convergence of the detonation contribute to the increased pressure of the shock wave generated in the powder. The detonation angle and the convergence of the detonation can be controlled separately. The computer simulations confirm this and show a good resemblance with the experimental results.

There is a regular reflection of the oblique detonation wave at the aluminum cylinder. The absence of a Mach reflection has been explained although its presence, in the case of a different detonation angle, would still mean that high pressures are generated in the powder.

ACKNOWLEDGMENT

The authors wish to acknowledge E. W. Koopmans and N. van der Heiden from the group Munition Effects and Ballistic Protection of the Prins Maurits Laboratory for their assistance with the flash x-ray photography.

[1] T. Z. Blazynski, *Dynamically Consolidated Composites: Manufacture and Properties* (Elsevier Applied Science, London, 1992).
[2] V. F. Nesterenko, S. A. Pershin, B. V. Farmakovskii, A. P. Khinskii, S. N. Zolotarev, N. A. Usishchev, and S. N. Novikov, Combust. Explos. Shock Waves **27**, 485 (1990).
[3] T. Akashi and A. K. Sawaoka, J. Mater. Sci. **22**, 1127 (1987).
[4] K. Kondo, S. Soga, and A. Sawaoka, J. Mater. Sci. **20**, 1033 (1985).
[5] L. E. Murr, *Shock Waves For Industrial Applications* (Noyes, New Jersey, 1988), Chap. 12.
[6] R. A. Graham and A. B. Sawaoka, *High Pressure Explosive Processing of Ceramics* (Trans. Tech., Switzerland, 1987), Chap. 8.
[7] Ref. 6, Chap. 6.
[8] Ref. 6, Chap. 5.
[9] National Materials Advisory Board, Report No. NMAB-394, 1983 (unpublished).
[10] S. DeCarli and M. A. Meyers, *Shock Waves and High-Strain-Rate Phenomena in Metals*, edited by Marc A. Meyers and Lawrence E. Murr (Plenum, New York, 1981), Chap. 22.
[11] Y. Horie and A. B. Sawaoka, in *Shock Compression Chemistry of Materials* (KtK Scientific, Tokyo, 1993), pp. 80–89.
[12] R. Prümmer, *Explosivverdichtung Pulverige Substanzen*, WFT 7, (Springer, Berlin, 1987), Chap. 5.
[13] M. A. Meyers and S. L. Wang, Acta Metall. **36**, 925 (1988).
[14] M. Held, Proceedings of EUROPYRO 1995, 6th International Congress on Pyrotechnics, June 1995, Tours, France (unpublished), pp. 185–191.
[15] R. Weinheimer, Proceedings of the 19th International Pyrotechnics Seminar, 1994 (unpublished), pp. 460–475.
[16] M. Adamec, B. S. Zlobin, and A. A. Shtertser, Combust. Explos. Shock Waves **27**, 385 (1991).
[17] P. Boogerd, Ph.D. thesis, Delft University, 1995.
[18] M. Cowperthwaite and W. H. Zwisler, *Tiger Computer Program Documentation* (SRI, Menlo Park, CA, 1973).
[19] N. K. Birnbaum, M. S. Cowler, M. Itoh, M. Katayama, and H. Obata, 9th International Conference on Structural Mechanics in Reactor Technology, Aug. 1987, Lausanne, Switzerland (unpublished).
[20] P. Boogerd, R. Verbeek, M. Stuivinga, A. C. Van der Steen, and J. Schoonman, J. Appl. Phys. **77**, 5077 (1995).
[21] N. S. Brar, Z. Rosenberg, and S. J. Bless, in *Shock Compression of Condensed Matter 1991*, edited by S. C. Schmidt, R. D. Dick, J. W. Forbes, and D. G. Tasker (Elsevier Science, Amsterdam, 1992), pp. 467–470.
[22] A. A. Shtertser, Combust. Explos. Shock Waves **24**, 610 (1987).
[23] R. H. Cole, in *Underwater Explosions* (Dover, New York, 1948), Chap. 2.
[24] N. A. Kostjukov, in *Shock Waves and High-Strain-Rate Phenomena in Metals*, edited by M. A. Meyers and L. E. Murr (Plenum, New York, 1981), pp. 843–49.
[25] Ch. Remiot, P. Chapron, and B. Demay, in *Shock Compression of Condensed Matter 1993*, edited by S. C. Schmidt, J. W. Shaner, G. A. Samara, and M. Ross (AIP Conference Proceedings, New York, 1994), Vol. 309, pp. 1763–1766.
[26] F. Jing, in *Shock Compression in Condensed Matter 1989*, edited by S. C. Schmidt, J. N. Johnson, and L. W. Davison (Elsevier Science, Amsterdam, 1990), pp. 33–44.
[27] P. Adroit, P. Chapron, and F. Olive, in *Shock Waves in Condensed Matter 1981*, edited by W. J. Nellis, L. Seaman, and R. A. Graham (AIP Conference Proceedings, New York, 1982), pp. 505–509.